sciendo

Polish Journal of Medical Physics and Engineering
The Journal of Polish Society of Medical Physics
ISSN 1898-0309, doi: 10.2478/pjmpe-2022-0011

June 2022
Vol 28, Issue 2

Scientific Paper

Implementation of the Sievert integral for the calculation of dose distribution around the BEBIG Co-60 high dose rate brachytherapy source

Castrol DUMENYA [1,ABCDEF,*], Francis HASFORD [1,2,ADEF], Samuel Nii Adu TAGOE [1,3,ABDEF], Evans Sasu[3,ABDEF], Mark POKOO-AIKINS [1,2,DEF,] Belinda Buermle ASAMANYUAH[4,1,DE], John Humphrey AMUASI[1,EF]

[1]*Department of Medical Physics, Graduate School of Nuclear and Allied Sciences, University of Ghana, Ghana*
[2]*Radiological and Medical Sciences Research Institute, Ghana Atomic Energy Commission, Ghana*
[3]*National Center for Radiotherapy and Nuclear Medicine, Korle Bu Teaching Hospital, Ghana*
[4]*Radiological Applications Department, Nuclear Regulatory Authority, Ghana*
[*]*Corresponding author: Castrol Dumenya; castroldumenya@yahoo.com*

(received 9 January 2022; revised 6 April 2022; accepted 20 April 2022)

Abstract

Introduction: In radiotherapy, a computerized treatment planning system (TPS) is used for performing treatment planning to estimate the dose distribution within a patient. To simplify the dose calculation, mathematical algorithms are employed. TG43 formalism is widely used for brachytherapy. Before the implementation of a particular dose calculation algorithm in clinical practice, it is imperative to acknowledge the limitations and uncertainties associated with the algorithm. Regarding this, outputs of the algorithm are compared to measurements or dose calculation approaches using simple source placement geometries. The manual dose calculation method has to be robust, straightforward, and devoid of complexities to reduce the likelihood of committing errors in the dose calculation process. A lot of manual dose calculation approaches have been proposed for Brachytherapy sources, but one needs to ascertain their reliability.

Material and methods: Considering this, the output of an HDRplus treatment planning system dedicated to brachytherapy treatment planning and using the TG43 formalism to calculate the dose distribution around a BEBIG Co-60 source was validated with Sievert integral dose calculation approach. Simple source placement geometries were created with the TPS using the universal applicator, LLA1200-20, selected from the applicator library, and doses at various equidistant points from the applicator calculated with the TPS and the Sievert integral. Various steps to enhance the efficacy of the Sievert integral approach have been outlined.

Results: The doses compared favourably well with deviations ranging from 0.03 – 10.51% (mean of 3.13%), and 0.03 – 5.63% (mean of 2.55%) for angles along the perpendicular bisector of the source, ranging from $0° < \theta < 70°$ and $0° < \theta < 48°$, respectively.

Conclusions: The Sievert integral breaks down at angles: $\theta \geq 60°$, and therefore, neglecting large angles, the Sievert integral would be an efficient, effective, and valid tool for quality control of the HDRplus TPS for the Co-60 source.

Keywords: dose calculation; high dose rate brachytherapy; cobalt-60; Sievert integral; BEBIG.

Introduction

In Brachytherapy (BT), dose calculation algorithms are the essential software components in a computerized treatment planning system (TPS). These modules are accountable for the correct estimation of the dose distribution within a patient and could be linked to treatment duration, which is influenced immensely by source calibration methods, the BT system used for the BT implant, and the source localization approach.

The feats attained in the provision of radiotherapy modality of cancer treatment may decline if not harmonized using arduous dose calculation models and algorithms.[1] Basically, it's because the efficiency and superiority of any TPS largely depend on the sort of algorithms employed at each diverse phase of the process of planning. Based on manufacturer preferences, several types of dose calculation algorithms are used in modern TPS, but the choice of dose computational algorithm should be based on its computational speed without compromising on accuracy.[2] The quality of the dose distribution representation of a good

© 2022 Authors — This is an open access article licensed under the Creative Commons Attribution-NonCommercial-NoDerivs License (http://creativecommons.org/licenses/by-nc-nd/4.0/).

Authors' contribution: A – Research concept and design, B – Collection and/or assembly of data, C – Data analysis and interpretation, D – Writing the article, E – Critical revision of the article, F – Final approval of the article.

algorithm depends strongly on the data or the parameters used by the algorithm.[3] The concurrence between the calculated and delivered dose is of great importance in radiotherapy since the accuracy of the absorbed dose based on prescription determines the clinical outcome.[4]

There is a dual function of dose calculation algorithms in the practice of radiotherapy; for plan enhancement in the process of treatment planning and for nostalgic comparison of the relationship between the available treatment parameters and clinical output.

It outlines two conjointly incompatible objectives of the particular dose calculation algorithm under consideration. To start with, the dose calculation algorithm has to be expeditious so as to facilitate the treatment planning process in a medically satisfactory time frame, and secondly, the outcome of the dose calculation has to be adequately accurate so that the establishment of the relationship between delivered dose and the clinical outcome remains consistent and significant. This has called for more review into the subject of dose calculation.[4]

There are different dose calculation algorithms that are used in brachytherapy. These are Monte Carlo, Superposition-Convolution model, Sievert Integral model, and the latest being the AAPM TG 43 formalism. The Sievert integral is a substitute for experimental or other dose calculation algorithms. This method basically involves dividing a line source into small elementary sources and applying the inverse square law and filtration corrections to each. It is an indispensable tool for dose rate calculations around brachytherapy sources, combining simplicity with equitable computational times, requires limited input data, and is computationally efficient. This gives the Sievert Integral an advantage over the Monte Carlo (MC) technique which requires a large volume of input data and longer computational time. The limitation of the Sievert integral not being accurate in predicting dose rate distributions around low energy isotopes will not be a problem in this research study because the source, in this case, is ^{60}Co.[5]

Various forms of the Sievert Integral algorithm have been used over the past nine decades. The Sievert Integral could be modified to correct for photon attenuation in tissue. The classical Sievert Integral model lumps the primary beam and scattered beam together, and this takes care of the effect of the inverse square law.

Modifications in the basic model of the Sievert integrals increase the accuracy significantly; nevertheless, there are still discrepancies between the output from the Sievert integral and other dose calculation algorithms.[5] This study seeks to obtain the dose distributions around the new BEBIG ^{60}Co source based on the version of the Sievert integral, where the source strength is specified in air kerma.[6] The results will then be compared to the output of the TG43 formalism in use for the HDRplus TPS (Eckert & Ziegler BEBIG GmbH, Germany) dedicated to BT treatment planning at the National Centre for Radiotherapy and Nuclear Medicine Department, Korle Bu Teaching Hospital (NCRNM, KBTH) of Ghana.

As part of quality assurance (QA) procedures for HDR brachytherapy, it is required to perform some calculations to estimate doses at specific points called control points (CPs) around the brachytherapy source. This is used to validate the output of the TPS to understand and acknowledge limitations associated with the use of the TPS; uncertainties relating to proximal distances have been recorded for ^{192}Ir sources.[7,8] Sievert integral, as stated earlier, is one of the methods which can be used to calculate the dose distributions around a brachytherapy source. Therefore, there is a need to validate this method for the HDRplus TPS in use for dose distribution determination for the new BEBIG ^{60}Co HDR Multisource afterloader brachytherapy machine (produced by Eckert & Ziegler BEBIG GmbH, Germany). The HDRplus TPS runs on the TG43 algorithm, and the afterloader machine uses ^{60}Co with the code name Co0.A86.

The goal of this study was to establish that the modified Sievert integral can be used as a quality assurance tool for the BEBIG HDR ^{60}Co brachytherapy source by comparing its output of the HDRplus. Therefore, in order to ensure the accuracy of the output from the treatment planning system, the coordinates in the universal applicator are compared to the dwell positions generated by the remote afterloader.

This study involved calculating dose distribution for a treatment plan, in a plane perpendicular to the longitudinal axis of a universal cylindrical applicator, with the multiple source dwell positions located in the applicator. A prescribed dose of 2 Gy would be delivered, and dose measurements were taken at twelve CPs. For each source dwell position, the dose will be normalised to a distance of 1 cm from the central axis. The resultant dwell times, which will automatically be calculated by the HDRplus, will equally be used in obtaining the dose values from the Sievert integral procedure. Other required parameters will be inputted into the dose calculation formalism under study, and the results will then be analysed.

Materials and methods

Sievert Integral Technique

The Sievert integral, **Equation 1**, introduced in 1921 by Professor Sievert, is a method that can be used to calculate the exposure rate around a linear brachytherapy source. The method is implemented by dividing the line source into small elementary sources and putting into consideration inverse square law (ISL) and filtration corrections to each of these sources:[6]

$$F(r,\theta) = \int_0^{\theta} e^{-x \sec\theta} d\theta \qquad \text{Eq. 1}$$

where the various symbols have their usual meaning, as originally stated by Sievert.[6]

However, for the purpose of this research, a modified version of the Sievert integral will be utilized, and the computations will be carried out in Cartesian coordinates. The variable *F(r,θ),* which represents the exposure rate, will also be replaced with *I(x,y).*[6]

For a source with the following parameters, the exposure rate *dI* at a point *P(x,y)* contributed by the source element of length *dx*, as shown in **Figure 1**, is given by:

$$dI(x,y) = \frac{A}{L} \cdot \Gamma \cdot dx \cdot \frac{1}{r^2} \cdot e^{-\mu' \cdot t \cdot \sec\theta} \quad \text{Eq. 2}$$

Where L = active length
t = filtration
A = activity
Γ = exposure rate constant
μ' = effective attenuation coefficient for the filter
Making substitution with the following **Equations 3**, **4** and **5**:

$$r = \text{y} \sec\theta \quad \text{Eq. 3}$$

$$x = \text{y} \tan\theta \quad \text{Eq. 4}$$

$$dx = \text{y} \sec^2\theta \, d\theta \quad \text{Eq. 5}$$

and integrating **Equation 2**, the exposure rate *I(x,y)* obtained for the whole source:

$$I(x,y) = \frac{A\Gamma}{Ly} \int_{\theta_1}^{\theta_2} e^{-\mu' \cdot t \cdot \sec\theta} d\theta \quad \text{Eq. 6}$$

Equation 6 takes after **Equation 1**, which is the general form of the Sievert integral. The above Sievert integral (**Equation 6**) may be evaluated by numerical methods, but this would not be done in the case of this research.

For a source with intensity specified in terms of exposure rate $\dot{X}_s$ at a specified distance, ***s***, far from the source (i.e., $s \gg L$), then the Sievert integral can be written as:

$$I(x,y) = \frac{\dot{X}_s \cdot s^2}{Ly} \cdot e^{\mu' t} \int_{\theta_1}^{\theta_2} e^{-\mu' \cdot t \cdot \sec\theta} d\theta \quad \text{Eq. 7}$$

The source strength used for this research is specified in air kerma strength, hence the Sievert integral model that will be implemented is:

$$I(x,y) = \frac{S_K}{Ly\left(\frac{\overline{W}}{e}\right)} \cdot e^{\mu' t} \int_{\theta_1}^{\theta_2} e^{-\mu' \cdot t \cdot \sec\theta} d\theta \quad \text{Eq. 8}$$

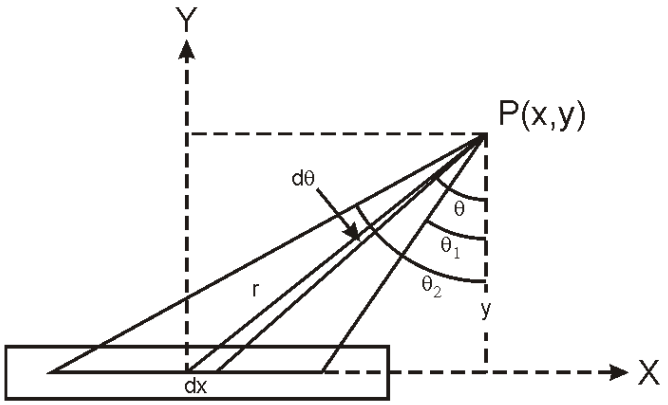

Figure 1. Diagram displaying the geometric relations used in the evaluation of exposure at point P, from an elementary source.[6]

Dose Calculation

Equation 8 calculates the exposure rate from the source, hence the need for conversion to dose. This was done by multiplying the emergent exposure rate expression by a quantity, f_{med}, or simply the *f-factor* which is sometimes called the roentgen-to-rad conversion factor. This factor is a constant dependent on the medium in which measurement is done (in this case, water) and the photon energy from the radioactive source. Tables containing the values of the f_{med} were referred to, and the value for a ^{60}Co photon energy, 1.25 MeV, in water is 37.6 Gy·kg/C.[6] Aside from the value of the constant being available in tables, the f_{med} can be calculated using **Equation 9** below.

$$f_{med} = 0.876 \frac{(\bar{\mu}_{en}/\rho)_{medium}}{(\bar{\mu}_{en}/\rho)_{air}} \quad \text{Eq. 9}$$

For a dimensional balance, the average work done per unit charge, $\frac{\overline{W}}{e}$, was converted from 0.876 cGy/R to cGy·kg/C using the factor:

$$1R = 2.58 \times 10^{-4} C/kg \quad \text{Eq. 10}$$

After the introduction of the *f-factor*, the resulting quantity is the dose rate. The dose is then calculated by multiplying the dose rate by the source dwell time (t_{dwell}) or treatment time which will be produced by HDR 3.0 Plus treatment planning system.

Equation 8 then becomes modified into **Equation 11** for calculation of the dose around the new BEBIG ^{60}Co source.

$$D = \frac{f_{med} \cdot S_K \cdot t_{dwell}}{L \cdot x \cdot \left(\frac{\overline{W}}{e}\right)} \cdot e^{\mu' t} \int_{\theta_1}^{\theta_2} e^{-\mu' \cdot t \cdot \sec\theta} d\theta \quad \text{Eq. 11}$$

The variable x in **Equation 11** has been used to replace y in **Equation 8** because the CP (point of measurement), unlike what is illustrated in **Figure 2**, is on the x or horizontal axis while the source is on the y or vertical axis.

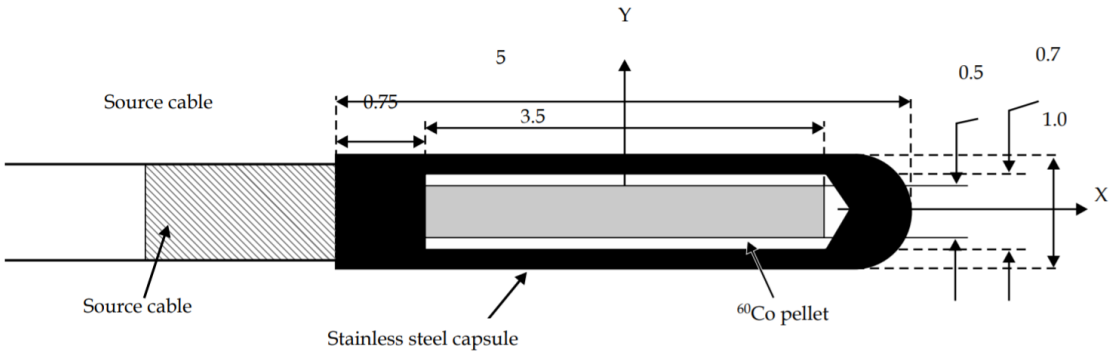

Figure 2. Schematic diagram of the new BEBIG Co-60 HDR brachytherapy source. [Reproduced from ref. 14, originally published under the terms of the CC BY-NC-SA 4.0 License (http://creativecommons.org/licenses/by-nc-sa/4.0/)]

Implementation of the Sievert Integral

An analytical solution of the Sievert integral does not exist; hence it will require either a numerical procedure or the use of a Sievert integral table of values such as that in appendix L. The Sievert integral in **Equation 11** has to be modified due to the difference in the definite interval between that in **Equation 11** $[\theta_1, \theta_2]$ and that used in the Sievert integral table $[0, \theta]$, which is identical to **Equation 1** and represented in **Equations 12** and **13**.

$$D_1 = \frac{f_{med} \cdot S_K \cdot t_{dwell}}{L \cdot x \cdot \left(\frac{W}{e}\right)} \cdot e^{\mu' t} \int_0^{\theta_1} e^{-\mu' \cdot t \cdot \sec\theta} d\theta \qquad \text{Eq. 12}$$

$$D_2 = \frac{f_{med} \cdot S_K \cdot t_{dwell}}{L \cdot x \cdot \left(\frac{W}{e}\right)} \cdot e^{\mu' t} \int_0^{\theta_2} e^{-\mu' \cdot t \cdot \sec\theta} d\theta \qquad \text{Eq. 13}$$

The variation in the angles under consideration in this research and those used in obtaining the integral values in the table, and the corresponding *x*-values were obtained through extrapolation and interpolation calculations. The *x* used in **Equation 11** differs from that in **Equation 1**. In comparison to that in **Equation 1**, the product of the effective attenuation coefficient, μ', calculated using **Equation 14** given by Williamson et al.[12], and the wall thickness, *t*, which is 0.05 cm, yielded the value of *x*.

$$\mu'(d) = -\left(\frac{1}{d}\right) ln \left[\frac{\sum_i p_i E_i \left(\frac{\mu_{en}}{\rho}\right)_i^{air} e^{-\mu_{en}^i \cdot d}}{\sum_i p_i E_i \left(\frac{\mu_{en}}{\rho}\right)_i^{air}}\right] \qquad \text{Eq. 14}$$

Where p_i = denotes the number of photons with energy E_i emitted per disintegration

$\left(\frac{\mu_{en}}{\rho}\right)_i^{air}$ = mass energy absorption coefficient in air for photon of energy E_i

d = filter thickness

E_i = photon energy

The value of the attenuation μ_{en} substituted into **Equation 14** to calculate the effective attenuation coefficient of the filter material for the source energy being considered, is the fitted value for the attenuation of the filter, μ_f = 0.25 cm^{-1}. This was to ensure accuracy in calculated values and minimise the deviations between the Sievert model and any other model it is compared to which in this case is the TG43 (Nath et al., 1995).[9] The other values for the attenuation are shown in **Table 1**.

Table 1. Actual and fitted values of linear attenuation coefficient for source and filtration materials μ_s and μ_f, respectively, for the new BEBIG source.[15]

Linear attenuation co-efficient	$\mu_s(cm^{-1})$	$\mu_f(cm^{-1})$
Actual value	0.47	0.43
Fitted values	0.25	0.25

The Sievert integral value for each angle, θ_1, and θ_2, were obtained individually, and the expression for their doses and a correction factor, calculated using the Meisbeger polynomial (**Equation 15**), were multiplied. The difference in the doses obtained for each angle yielded the dose at the specified control point. All calculations were done using by a MATLAB program.

$$M_{poly} = A + Br + Cr^2 + Dr^3 \qquad \text{Eq. 15}$$

$$r = \sqrt{x^2 + y^2} \qquad \text{Eq. 16}$$

Where M_{poly} = Meisberger polynomial/function

r = distance from the source to control point calculated using x and y values

A, B, C and D are constants or polynomial coefficients whose values are source dependent and for ^{60}Co:

A = 0.99423 Eq. 17

B = -0.005318 Eq. 18

C = -0.002610 Eq. 19

D = 0.0001327 Eq. 20

BEBIG ^{60}Co Source

The radioisotope used for this research is ^{60}Co, and its details are given in **Table 2**. The Eckert & Ziegler BEBIG Co-60 source is loaded with an activity of about 81.4 GBq. The capsule design of the source fulfils the demanding regulatory and governmental standards of the EU and other nations. The capsule and source wire are connected by high-quality laser welding method and crafted to withstand 100,000 source transfers. This has been verified by stress tests in straight and curved applicators exceeding this figure to ensure safety and long-term precision. With a value of 100,000 cycles in a period of five years, the brachytherapy unit of a clinic could have an estimate of up to seven patients a day receiving a ten channel interstitial treatment or twenty-four patients a day for the treatment with a three-channel applicator.

Table 2. Details of the BEBIG ^{60}Co source including some initial parameters and their corresponding values.

Parameter	Value	
Source Name	Multisource Co-60 HDR	
Radionuclide	Co-60	
Model Number	Co0.A86	
Serial Number	BB-AC 547	
	Initial values	**Activity for planning**
Air KERMA Strength	23210 cGy·cm^2/h	16343.6 cGy·cm^2/h
Activity in GigaBecquerel	78.85 GBq	53.41 GBq
Activity in Curie	2.05 Ci	1.4435 Ci

The new model of the BEBIG ^{60}Co HDR (model Co0.A86) brachytherapy source design has a small active core with a diameter of 0.5 mm and a more rounded capsule tip as compared to the old BEBIG source design. Its central cylindrical active core length is 3.5 mm which is made of metallic ^{60}Co. This active core is covered by a cylindrical stainless steel capsule with an external diameter of 1.0 mm (more details are given in **Figure 2**).

Treatment Planning System (TPS)

The TPS used in the simulation of the sources is the HDRplus manufactured by BEBIG. It provides treatment comfort due to its user-friendly interface; it's fast, flexible, precise, and delivers an optimised treatment plan. The HDRplus supports all HDR applications, including intracavitary, interstitial and intraoperative treatments.

Its user interface features an ultramodern and easy-to-use structure with the many options to customise the layout and parameter settings which further allows the user to decide on a personal planning approach. Another unique feature of the HDRplus is the complete applicator database which is used to select applicators and place them directly on an X-ray film or CT/MR images which eliminates the procedure of lengthy reconstruction of the applicator. The automated nature of the applicator reconstruction makes the HDRplus to identify implanted needles and visualise them in 3D for simplification of the treatment planning. Automatic image fusion feature of this treatment planning system enables its users to match CT and MR images without any user interference within a time frame of less than 30 seconds.

The version of the HDRplus TPS used for the procedure is version 3.0.5. The software was launched from the desktop of the system, and a patient profile with the name "Sievert integral" was created. The universal applicator with a dimension of 12 cm and the name LLA1200-20 was selected, and a (0, 0) dose plane was defined on the orthogonal view. The origin was also defined, i.e., (0, 0) point, and the midpoint, 5.5 cm of the source location in the applicator was placed on the (0, 0) point.

CPs were generated with a spacing of 1 cm apart on the *x*-axis to the left and right of the *y*-axis. A prescribed dose of 2 Gy was normalised to the x = 1 cm CP, which is the first point from the origin. The TPS generated a dose distribution, and the doses to the various CPs were recorded. The same procedure was repeated for the (0, 1), (0, 2), (0, -1) and (0, -2) cm points.

AAPM TG 43 Dose Calculation Formalism

The TG43 report[9,10] recommended the dose calculation algorithm for establishing the two-dimensional dose rate distribution in a water medium around a cylindrically symmetric photon-emitting brachytherapy source. The TG 43 formalism is a more advantageous method because it contains quantities or parameters measured solely in the medium. The data for a specific source can be compiled as a function of position, and the effects of several physical factors on the value of the dose rate distribution are considered separately.[11]

Comparison of Sievert Integral Values and HDRplus Results

The dose obtained from the two methods was analysed by producing curves of dose against control points for each dwell position. The graphical representations were utilized for a clearer view of the deviation of the outcomes of the two procedures.

Percentage deviations of the Sievert integral dose values from that of the HDRplus, which was designed based on the TG 43 algorithm, were calculated using the relation

$$\%\, Deviation = \frac{|D_{SI} - D_{HDRplus}|}{D_{HDRplus}} \times 100\ \% \qquad \text{Eq. 21}$$

Where D_{SI} = Dose from Sievert integral
$D_{HDRplus}$ = Dose from HDRplus

Results

HDRplus Dose Computations

The acquired results for the individual control points are shown in the **Table 3** and the corresponding isodose lines in **Figure 3**.

Sievert Integral Results

The computations from the Sievert integral yielded results recorded in tables for each control point. The dose outcome to control points equidistant and at equal subtended angles from the source, which were to the left and right of the source were equal. Therefore, *x* values represented in the following tables, for this section, are the absolute values of *x*.

The Sievert integral could not be used in calculating dose delivered to various control points when the source was positioned at the perpendicular bisector, i.e. at (0, 0), and this was because the angle or value of θ is equal to zero.

The means doses recorded at each control point with equal distance and oblique directions from the source were calculated to carry out comparison between obtained dose values from both methods under consideration. Tables of values showing both sets of dose values for each source dwell position and the corresponding deviations. The following curves, in **Figure 4 (a-d)**, were obtained to visualise how clearly the two methods' dose outcome deviate from each other with respect to the control points.

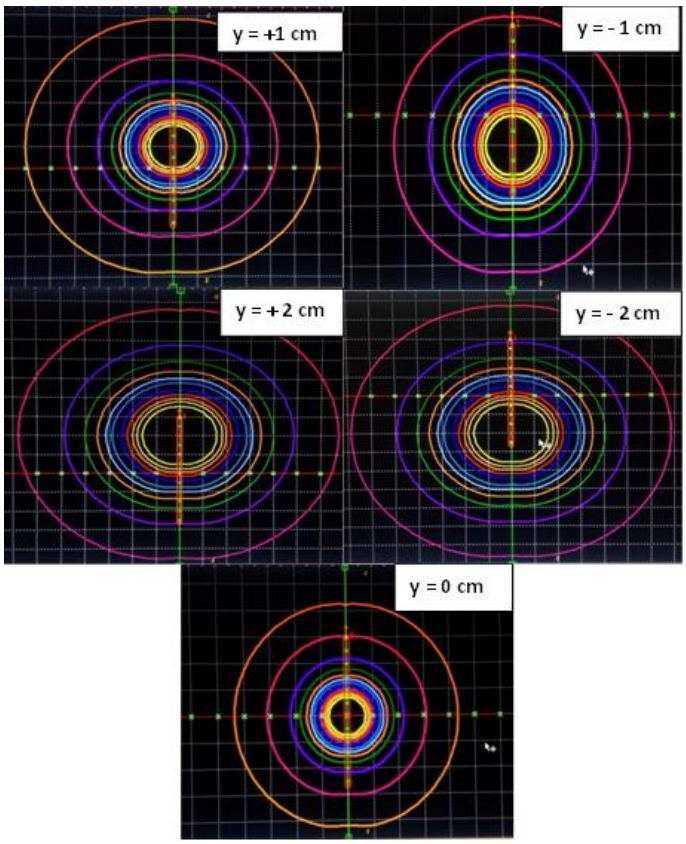

Figure 3. Isodose lines for the Co-60 Source at various y-positions and interface of the HDRplus.

Table 3. CP parameters for source at various y values

	y-axis positions (cm)				
	-2	**-1**	**0**	**+1**	**+2**
Prescribed Dose (Gy)	2.00	2.00	2.00	2.00	2.00
Total Dwell Time (s)	208.64	81.81	40.25	78.68	202.72
Dwell Position co-ordinates (cm)	(0,-2)	(0,-1)	(0,0)	(0,1)	(0,2)
Total Reference Air Kerma (cGy·m^2)	0.09472	0.03714	0.01827	0.03572	0.09203
Minimum Dose (Gy)	0.24	0.1	0.05	0.1	0.23
Average Dose (Gy)	0.85	0.61	0.49	0.6	0.84
Maximum Dose (Gy)	2.01	2.01	2.00	2.00	2.00

Table 4. Comparison of dose values for both methods for source at y = ±1cm

y = -1 cm			**y = +1 cm**		
Sievert_Dose (Gy)	**HDR_Plus_Dose(Gy)**	**% Deviation**	**Sievert_Dose(Gy)**	**HDR_Plus_Dose(Gy)**	**% Deviation**
1.9793	2.0050	1.28	1.9036	1.9950	4.58
0.7905	0.7900	0.06	0.7603	0.7800	2.53
0.3901	0.3900	0.03	0.3752	0.3800	1.26
0.2256	0.2300	1.91	0.2170	0.2200	1.36
0.1442	0.1500	3.87	0.1386	0.1400	1.00
0.0990	0.1000	1.00	0.0953	0.1000	4.70

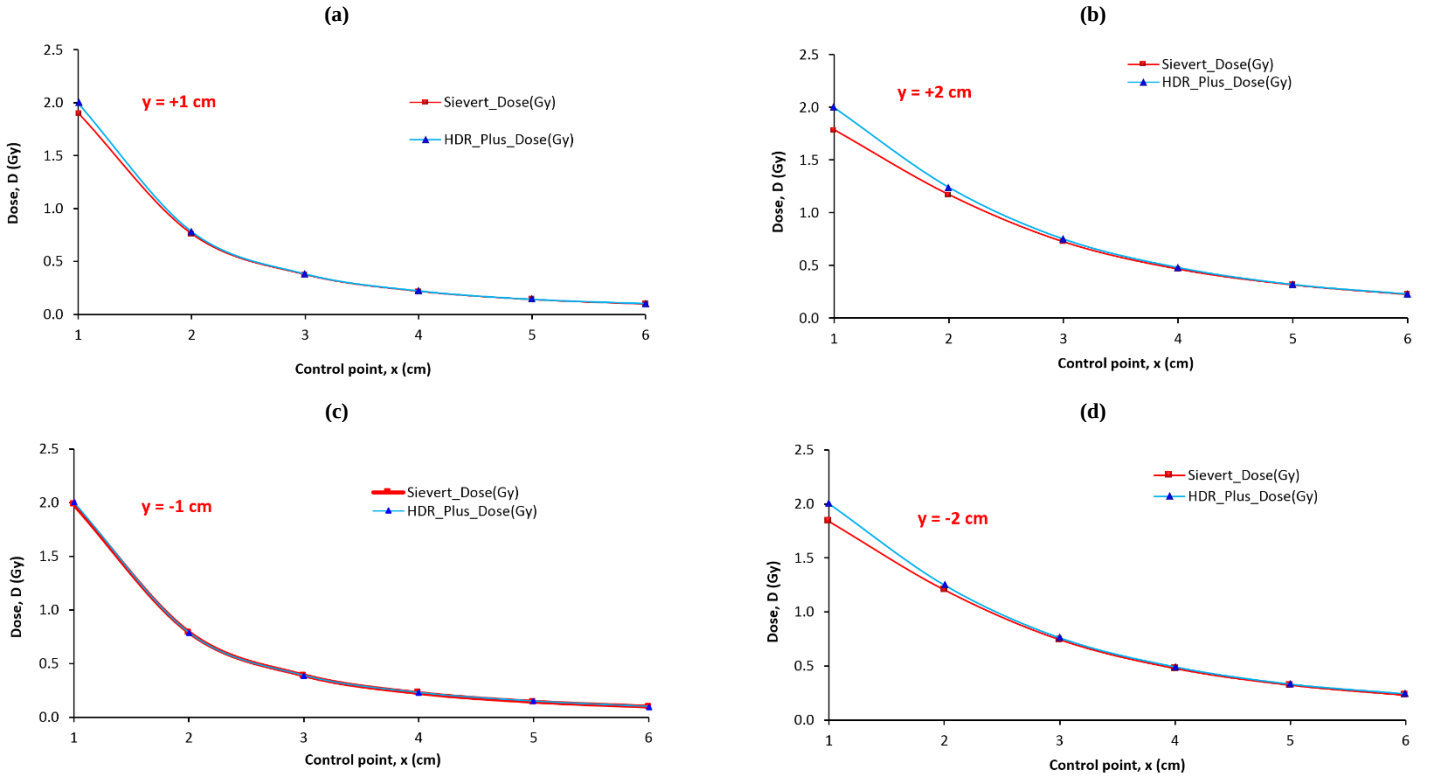

Figure 4. Curves to compare dose outputs for source at (a) y = 1cm (b) y = +2cm (c) y = -1 cm (d) y = -2 cm

Discussion

The observations made from the results obtained from the TPS clearly showed a generally good agreement in dose values for points with the same distance and oblique directions from the source. However, this was not the case for the x = 1 cm control point (CP) readings for the source at the (0, -2), (0, -1), (0, 1) and the (0, 2) cm x-y co-ordinate location. The 100% mark to which the dose normalisation to x = 1 cm was done was only achieved for the scenario where the source was positioned at the perpendicular bisector or at the (0, 0) location, while a dose percentage of 99.5% and 99.6% of the prescribed 2 Gy was recorded for the (0, 1) and (0, 2) cm source dwell-positions respectively. When the source was positioned at the (0, -1) and (0, -2) cm dwell positions, the dose percentage, normalized to the 2 Gy prescribed, recorded was 100.5% and 100.4%, respectively. These deviations from the expected outcome (100%) could be attributed to the influence of the encapsulation design, as shown in **Figure 2**. The non-uniformity in the distance from the core of the sealed source to the external part of the capsule could have resulted in the slight increase in distance of the Co-60 Source from the CP. Low discrepancies in dose values for equidistant and equiangular points were expected, but the greater thickness of the head of the capsule could have contributed to this variation, and this resulted in the increment in the source dwell-time when the source was positioned below the perpendicular bisector. This is because the shielding of the source was greater, hence a greater treatment time, 81.81 seconds for (0, -1) cm and 208.64 seconds for (0, -2) cm, was required to attain the prescribed dose as compared to the 78.68 seconds and 202.72 seconds used for the (0, 1) cm and (0, 2) cm respectively.

The Sievert integral technique was incapable of calculating the dose for the source positioned at (0, 0) cm because the angle subtended with reference to the CPs was 0°. However, it calculated the dose for all other source dwell positions, producing dose values that were in acceptable ranges in comparison to what was expected. Early approximations and rounding off of figures resulted in an increment in the error produced; hence the decision to work with figures with at least four places of decimal to increase the accuracy of produced results, and further reduces the percentage deviation. The simplicity and speed of the MATLAB program utilised in carrying out the calculations enabled the dose computations per control point to take an average period of 30 seconds. Also, the magnitude of x and y values were used in the computations to produce positive dose values (as a negative dose value would be meaningless); hence the dose value for CPs equidistant and equiangular from the source dwell-position were equal.

The general agreement in the dose output at CPs equidistant and equiangular for both methods resulted in the use of the mean of the doses from each pair of points to compare and analyse the results. The dose outputs from both methods were generally close with minimal percentage deviations. It was observed that for extreme oblique directions, the percentage deviation of the Sievert integral dose output from the TG43-based HDRplus TPS

was larger as compared to points of lesser angular value. This verifies what Williamson et al[12] established, that the Sievert approach introduces significant errors and practically breaks down in the extreme oblique directions.

With the exception of very high deviations obtained from the extreme oblique directions, the Sievert integral dose output for the Co-60 has shown to be a reliable method to perform a quality control on the HDRplus TPS. This is evident in the overlap of the curves plotted for dose against distance for both methods, most especially for the (0, -1) cm source dwell position.

The deviations recorded for the (0, -1) cm dwell position had a range of 0.03 – 3.87% as compared to its counterpart, i.e., (0, 1) cm dwell position with a range of 1.00 – 4.70% could be used to assume that the Sievert integral produces much accurate dose values with a higher treatment time. This could be confirmed with the range for the (0, 2) cm and (0, -2) cm dwell position.

Following the ICRU report[13] that the percentage deviation of dose values calculated should not exceed ±5% of the true value, the Sievert integral has proven to be a valid tool for quality control of the HDRplus using the range with less error. Also, for purposes of radiation protection and patient safety, the TG43 formalism has shown superiority because the Sievert integral required more exposure or treatment time to yield the expected dose in most cases.

Conclusions

The model of the Sievert integral used in this research alongside the approximations applied, i.e., the Meisberger polynomial, has shown to be a valid model to calculate the dose distribution around the new BEBIG Co-60 except for extreme oblique directions, where it appears to break down. The percentage deviation range of the dose output from the Sievert integral in comparison to that of the output from the TPS is 0.03 – 10.51%, with a mean of 3.13% for the angle range of $0° < \theta < 70°$. The Sievert integral broke down at respectively large angles, which in this case was from above 60°. Therefore, neglecting the breaking point, i.e., $\theta \geq 60^{o}$, the range becomes 0.03 – 5.63% with a mean value of 2.55% for the angle range of $0° < \theta < 48°$.

References

1. Papanikolaou N, Stathakis S. Dose-calculation algorithms in the context of inhomogeneity corrections for high energy photon beams. Medical Physics. 2009;36(10):4765-4775. https://doi.org/10.1118/1.3213523
2. Kyeremeh P, Addison E, Acquah G, et al. Implementation of 3-D Anisotropy Corrected Fast Fourier Transform Dose Calculation around Brachytherapy Seeds. International Journal of Science and Technology. 2012;2(3):116-124.
3. Animesh. Advantages of multiple algorithm support in treatment planning system for external beam dose calculations. Journal of Cancer Research and Therapeutics. 2005;1(1):12-20. https://doi.org/10.4103/0973-1482.16085
4. Oelkfe U, Scholz C. Dose Calculation Algorithms. In: New Technologies in Radiation Oncology. Springer; 2006:187-196. https://doi.org/10.1007/3-540-29999-8_15
5. Nani EK, Akaho EHK, Kyere AWK, et al. Approximating Sievert Integrals to Monte Carlo Methods to Calculate Dose Rate Distributions around P192PIr Brachytherapy Source. Journal of Applied Science and Technology. 2009;14(1-2):27-31. https://doi.org/10.4314/jast.v14i1-2.44320
6. Khan FM. The Physics of Radiation Therapy. 3rd ed. Lippincott Williams & Wilkins; 2003:369-377.
7. Daskalov GM, Löffler E, Williamson JF. Monte Carlo-aided dosimetry of a new high dose-rate brachytherapy source. Medical Physics. 1998;25(11):2200-2208. https://doi.org/10.1118/1.598418
8. Cohen GN, Amols HI, Zaider M. An independent dose-to-point calculation program for the verification of high-dose-rate brachytherapy treatment planning. International Journal of Radiation Oncology, Biology, Physics. 2000;48(4):1251-1258. https://doi.org/10.1016/s0360-3016(00)00725-2
9. Nath R, Anderson LL, Luxton G, Weaver KA, Williamson JF, Meigooni AS. Dosimetry of interstitial brachytherapy sources: Recommendations of the AAPM Radiation Therapy Committee Task Group No. 43. Medical Physics. 1995;22(2):209-234. https://doi.org/10.1118/1.597458
10. Rivard MJ, Coursey BM, DeWerd LA, et al. Update of AAPM Task Group No. 43 Report: A revised AAPM protocol for brachytherapy dose calculations. Medical Physics. 2004;31(3):633-674. https://doi.org/10.1118/1.1646040
11. Kyeremeh PO. Three-Dimensional Implementation of Anisotropy Corrected Fast Fourier Transform Dose Calculation around Brachytherapy Seeds. (MPhil Thesis). University of Ghana, Accra, Ghana. Published online 2011.
12. Williamson JF, Morin RL, Khan FM. Monte Carlo evaluation of the Sievert integral for brachytherapy dosimetry. Physics in Medicine and Biology. 1983;28(9):1021-1032. https://doi.org/10.1088/0031-9155/28/9/002

13. International Commission on Radiation Units and Measurements. Determination of Absorbed Dose in a Patient Irradiated by Beams of X or Gamma Rays in Radiotherapy Procedures. International Commission on Radiation Units and Measurements ICRU Report 24; 1976.
14. Zehtabian M, Sina S, Rivard MJ, Meigooni AS. Evaluation of BEBIG HDR 60 Co system for non-invasive image-guided breast brachytherapy. Journal of Contemporary Brachytherapy. 2015;7(6):469-478. https://doi.org/10.5114/jcb.2015.56766
15. Bhola S, T Palani Selvam, Sridhar S, Vishwakarma RS. An analytic approach to the dosimetry of a new BEBIG 60 Co high-dose-rate brachytherapy source. Journal of Medical Physics. 2012;37(3):129. Accessed January 9, 2022. https://dx.doi.org/10.4103%2F0971-6203.99228